Rare Metal Materials and Engineering
Volume 50, Issue 5, May 2021
Available online at www.rmme.ac.cn

Science Press

Cite this article as: Xu Jianyan, Kong Dejun. Tribological Characteristics of Laser Thermal Sprayed $Co_{30}Cr_8W_{1.6}C_3Ni_{1.4}Si$ Coating in PAO+2.5%MoDTC Oil[J].Rare Metal Materials and Engineering, 2021, 50(05): 1542-1548.

ARTICLE

Tribological Characteristics of Laser Thermal Sprayed $Co_{30}Cr_8W_{1.6}C_3Ni_{1.4}Si$ Coating in PAO+2.5%MoDTC Oil

Xu Jianyan, Kong Dejun

College of Mechanical Engineering, Changzhou University, Changzhou 213164, China

Abstract: To elevate the wear resistance of TC4 alloy, $Co_{30}Cr_8W_{1.6}C_3Ni_{1.4}Si$ coating was fabricated on the surface by laser thermal spraying (LTS). The morphologies and phases of obtained coatings were analyzed by scanning electronic microscope (SEM) and X-ray diffraction (XRD), respectively. The friction and wear properties of the coatings in poly-alpha-olefin (PAO)+2.5wt% molybdenum dithiocarbamate (MoDTC) oil were investigated by wear tester. The results show that the laser thermal sprayed $Co_{30}Cr_8W_{1.6}C_3Ni_{1.4}Si$ coatings are primarily composed of Ti, WC_{1-x}, CoO, Co_2Ti_4O and CoAl phases, and the metallurgical bonding forms at the coating interface. The average coefficient of friction (COF) of $Co_{30}Cr_8W_{1.6}C_3Ni_{1.4}Si$ coatings fabricated at the laser power of 1000, 1200 and 1400 W is 0.151, 0.120, and 0.171 with corresponding wear rate of 1.17×10^{-6}, 1.33×10^{-6} and 2.80×10^{-6} $mm^3\cdot N^{-1}\cdot m^{-1}$, respectively, which increases with the increase of laser power. The wear mechanism is abrasive wear, and the dendrite size is the dominant role of anti-wear.

Key words: laser thermal spraying (LTS); $Co_{30}Cr_8W_{1.6}C_3Ni_{1.4}Si$ coating; PAO+2.5wt% MoDTC oil; coefficient of friction (COF); wear mechanism

TC4 alloy has been extensively used in the fields of aeronautical manufacture, chemical industry and ocean engineering due to its high strength and excellent corrosion resistance[1-3]. However, its poor tribological performance affects the service life in engineering applications[4,5]. The surface technologies, such as laser thermal spraying (LTS), physical vapor deposition (PVD) and chemical vapor deposition (CVD), have been used to enhance the hardness[6-8] and effectively improve the friction and wear performances of TC4 alloy. Among the mentioned techniques, the LTS-fabricated coatings on TC4 alloy have advantages of dense structure and strong metallurgical bonding with the substrates[9-11]. Researchers found that the self-fluxing alloys as the spraying powders can further improve the tribological performance of laser cladded coatings. Zhao et al[12] investigated the wear performance of Co-based alloy coating fabricated by laser cladding, and found that the wear resistance is enhanced 3.6~6.2 times as that of primary substrate. Yan et al[13] revealed that the wear properties of Co-based alloy/TiC/CaF_2 self-lubricating coatings have good friction-reduction and anti-wear abilities at ~ 400 °C. Li et al[14] revealed that the hardness of Co-based alloy coating increases 2.3 times as that of substrate. The above results show that the Co-based alloy coatings on TC4 alloy can improve the friction-reducing and anti-wear performances.

As an organic Mo antifriction, molybdenum dithiocarbamate (MoDTC) is widely added into the poly-alpha-olefin (PAO) in the friction-reduction field, which can activate the tribochemical reactions to enhance the friction performance. The friction-reduction caused by Mo oxide derived from the MoDTC improves the lubrication performance[15]. Despite the Co-based alloy coating has excellent friction-reduction performance, the friction and wear behavior of laser thermal sprayed $Co_{30}Cr_8W_{1.6}C_3Ni_{1.4}Si$ coatings in PAO+2.5wt% MoDTC oil has barely been reported.

In this study, the effects of laser power on the friction and wear behavior of laser thermal sprayed $Co_{30}Cr_8W_{1.6}C_3Ni_{1.4}Si$

Received date: May 20, 2020
Foundation item: Key Research and Development Project of Jiangsu Province (BE2016052)
Corresponding author: Kong Dejun, Ph. D., Professor, College of Mechanical Engineering, Changzhou University, Changzhou 213164, P. R. China, Tel: 0086-519-81169810, E-mail: kong-dejun@163.com

coatings in PAO+2.5wt% MoDTC oil were investigated, which provides an experimental basis in the tribological field for TC4 alloy.

1 Experiment

1.1 Sample preparation

The substrate was the commercial TC4 alloy with the chemical composition as follows: 5.5wt%~6.8wt% Al, 3.5wt% ~4.5wt% V, 0.3wt% Fe, 0.15wt% Si, 0.10wt% C, 0.15wt% N, 0.05wt% H, 0.20wt% O, and Ti. The TC4 alloy was mechanically sandblasted with sandpaper of 600#, 800# and 1000#, cleaned ultrasonically with alcohol, and then dried in the air. The PAO+2.5%MoDTC oil consisted of 97.5wt% PAO and 2.5wt% MoDTC. PAO was selected as the based oil, and its physical-chemical parameters are: viscosity of 16.68 $mm^2 \cdot s^{-1}$, flash point of 213 °C, pour point of −72 °C, viscosity index of 124, and evaporation loss of 11.8%. The additive was MoDTC, and its physical-chemical parameters are: density of 1.01 $g \cdot cm^{-3}$, viscosity of 700 $mm^2 \cdot s^{-1}$, flash point of 135 °C, Mo content of 10.0wt% and S content of 11.0wt%.

The LTS test was conducted in a fiber-coupled laser spraying system with the spot diameter of 5 mm, powder feeding speed of 8 $g \cdot min^{-1}$, laser scanning speed of 30 $mm \cdot s^{-1}$, and laser power of 1000, 1200 and 1400 W.

1.2 Characterization methods

The surface and cross-section morphologies of obtained coatings were analyzed by a JSM-6360LA type scanning electronic microscope (SEM), and the phases were analyzed using a D/max2500PC type X-ray diffraction (XRD). The hardness was measured five times using a XHV-1000T type hardometer with load of 0.1 N and dwell time of 10 s.

The friction and wear test was carried out on a CFT-I type friction and wear tester. The coating was immersed in PAO+ 2.5%MoDTC oil with the load of 20 N at 25 °C for 30 min and the tribo-pair is Si_3N_4 balls with the diameter of 3.5 mm and sliding length of 4 mm.

The morphologies, element distributions and phases of worn tracks were investigated by SEM, energy dispersive spectrometer (EDS) and XRD, respectively. The profiles of worn tracks were analyzed using a VHX-700FC type super-deep three-dimensional microscope.

Wear rate was calculated by Eq.(1):

$$W = \frac{K_b}{PL} \tag{1}$$

where K_b is the wear volume, μm^3; P is the wear load, N; L is the width of worn track, m.

2 Results and Discussion

2.1 Morphology and XRD analyses of powder

Fig.1a shows the morphology of $Co_{30}Cr_8W_{1.6}C_3Ni_{1.4}Si$ powder. The powder is irregular spheroidal particles with the size of 80~100 μm accompanied by some fine particles. It can be seen that no agglomerated particle exists, which is favorable for the powder feeding in the LTS process. Fig.1b shows the XRD pattern of the powder. The $AlCr_2$, $CrSi_2$, Co_3Ti, AlCo,

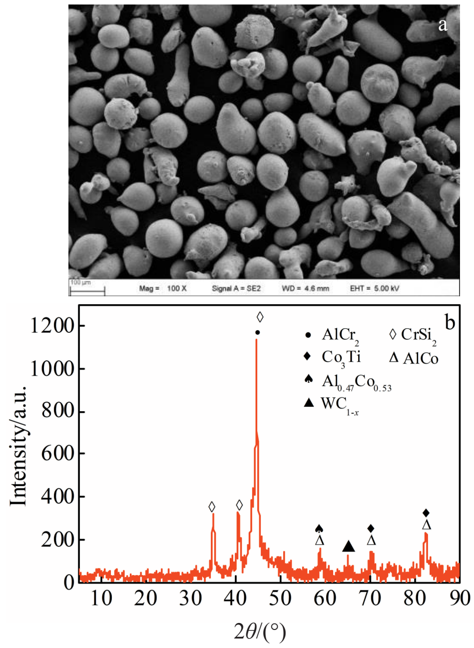

Fig.1 Morphology (a) and XRD pattern (b) of $Co_{30}Cr_8W_{1.6}C_3Ni_{1.4}Si$ powder

$Al_{0.47}Co_{0.53}$ and WC_{1-x} peaks are detected, indicating that the powder is composed of Co, Cr, W, C, Ni and Si without impurity elements.

2.2 Characterization of coating surface

2.2.1 Morphologies and XRD analyses of coating surface

Fig.2a_1 shows the surface morphology of $Co_{30}Cr_8W_{1.6}C_3Ni_{1.4}Si$ coating fabricated at the laser power of 1000 W. The black and tiny dendrites are uniformly distributed in the coating, with no porosity or crack defect. The coating is composed of Ti, WC_{1-x}, CoO, Co_2Ti_4O and CoAl phases, and the oxides of Co and Ti come from the partial oxidation in the coating, as shown in Fig.2a_2.

Fig. 2b_1 shows the surface morphology of $Co_{30}Cr_8W_{1.6}C_3$-$Ni_{1.4}Si$ coating fabricated at the laser power of 1200 W. The dendrites are lager and darker than those fabricated at the laser power of 1000 W. The coating is also composed of Ti, WC_{1-x}, CoO, Co_2Ti_4O and CoAl phases, and the peak intensity increases with the increase of laser power, as shown in Fig.2b_2.

Fig. 2c_1 shows the surface morphology of $Co_{30}Cr_8W_{1.6}C_3$-$Ni_{1.4}Si$ coating fabricated at the laser power of 1400 W. The black dendrites become bigger and darker than those fabricated at the laser power of 1000 and 1200 W, because the increase of laser power promotes the growth of dendrites. The phase composition of coating is the same as that fabricated at the laser power of 1200 W, as shown in Fig.2c_2.

From the above analyses, it can be seen that the dendrites become lager and darker with the increase of laser power, because the higher laser power leads to the following effects: (1) the diffusions between the coating and the substrate strengthen, which is beneficial to forming the metallurgical bonding at the interface; (2) the excessive heat input causes

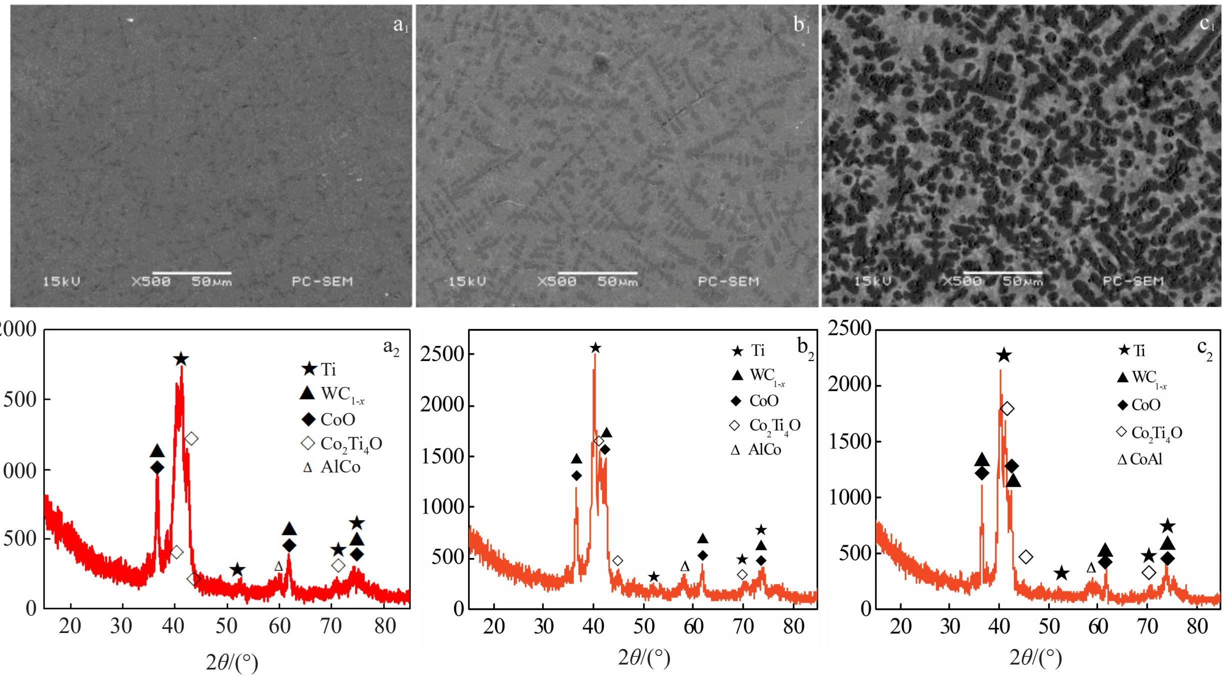

Fig.2 Morphologies (a_1, b_1, c_1) and XRD patterns (a_2, b_2, c_2) of $Co_{30}Cr_8W_{1.6}C_3Ni_{1.4}Si$ coating surfaces fabricated at laser power of 1000 W (a_1, a_2), 1200 (b_1, b_2) W and 1400 W (c_1, c_2)

the increase of superheat and slows the heat transfer process, resulting in the grain growth and decrease of the mechanical property of coating.

2.2.2 Hardness analysis

Hardness is an important index to valuate the coating quality, which has a close correlation with the wear resistance and service life of coating[16]. Fig.3 shows the average hardness of $Co_{30}Cr_8W_{1.6}C_3Ni_{1.4}Si$ coatings fabricated at different laser powers. The hardness of coatings fabricated at the laser power of 1000, 1200 and 1400 W is 12 710, 10 490, and 9790 MPa, respectively, which is higher than the hardness of substrate (3400 MPa), showing that the coating hardness gradually decreases with the increase of laser power which is attributed to the dendrite growth under the condition of high laser power.

2.2.3 Cross-sectional morphologies of coatings

Fig. 4 shows the cross-sectional morphologies of $Co_{30}Cr_8W_{1.6}C_3Ni_{1.4}Si$ coatings fabricated at different laser powers. The bonding line indicates the metallurgical bonding feature with no defects at the interface, because the coating and the surface layer of substrate melt and solidify to form the interdiffusion layer[17]. The thickness of coatings fabricated at the laser power of 1000, 1200 and 1400 W is about 900, 1200 and 1000 μm, respectively. The diffusion degree strengthens with the increase of laser power, which forms the metallurgical bonding at the coating interface.

2.3 Coefficient of friction and worn profiles

Fig. 5a shows the coefficients of friction (COFs) of $Co_{30}Cr_8W_{1.6}C_3Ni_{1.4}Si$ coatings fabricated at the different laser powers. The COFs in the running-in period are ~0.2, and then decrease to ~0.1 at the wear time of 4 min, indicating that the coatings

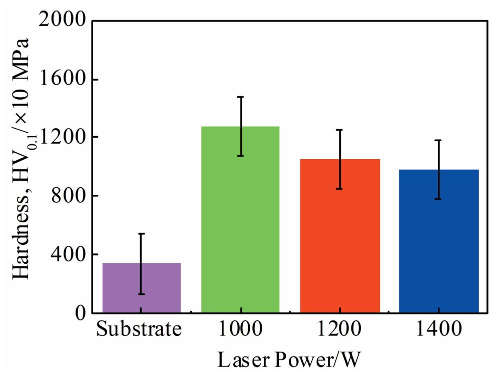

Fig.3 Hardness of $Co_{30}Cr_8W_{1.6}C_3Ni_{1.4}Si$ coatings fabricated at different laser powers

possess superior friction-reduction effect in PAO+2.5%MoDTC oil. The average COFs of coatings fabricated at the laser power of 1000, 1200 and 1400 W are 0.151, 0.120, and 0.171, respectively, which is lower than that of substrate (0.201). The COF variations of coatings fabricated at the laser power of 1200 and 1400 W are more obvious than those of coating fabricated at the laser power of 1000 W, because the severe adhesive wear occurs in the friction test.

The profiles of worn tracks and wear rates of coatings fabricated at different laser powers are shown in Fig.5b and 5c, respectively. The wear rate of $Co_{30}Cr_8W_{1.6}C_3Ni_{1.4}Si$ coatings fabricated at the laser power of 1000, 1200 and 1400 W is 1.17×10^{-6}, 1.33×10^{-6} and 2.80×10^{-6} $mm^3\cdot N^{-1}\cdot m^{-1}$, respectively, while that of the substrate is 4.31×10^{-6} $mm^3\cdot N^{-1}\cdot m^{-1}$, showing

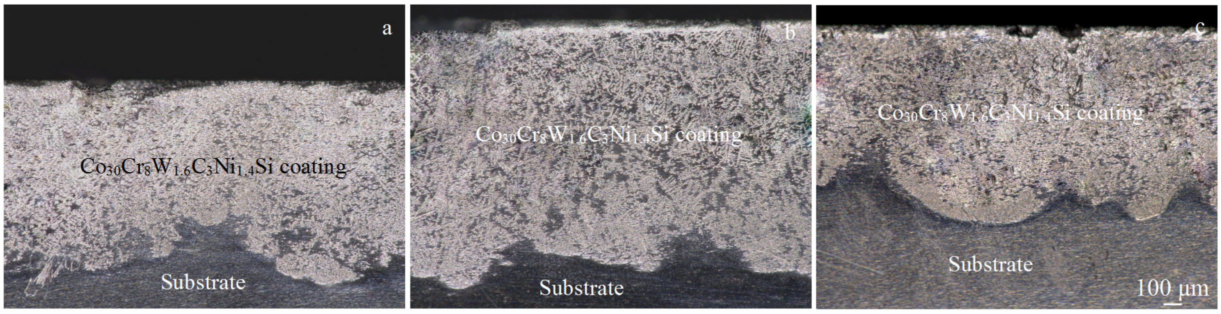

Fig.4 Cross-sectional morphologies of $Co_{30}Cr_8W_{1.6}C_3Ni_{1.4}Si$ coating fabricated at laser power of 1000 W (a), 1200 W (b) and 1400 W (c)

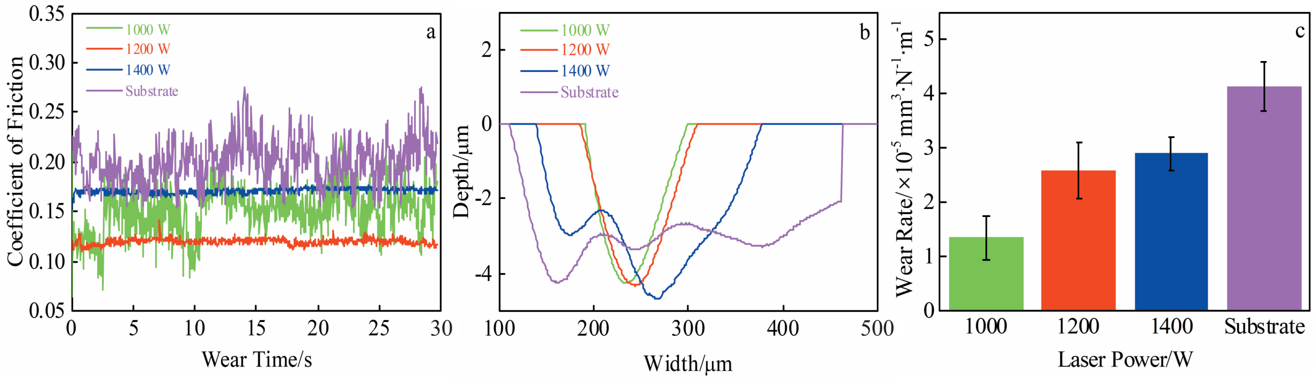

Fig.5 Coefficients of friction (a), profile of worn tracks (b) and wear rates (c) of substrate and coatings fabricated at different laser powers

that the coatings have significant wear resistance. This is because the larger heat input induced by the high laser power causes more substrate materials dissolved into the coating to decrease the coating hardness.

2.4 EDS analyses of worn tracks

Fig.6a and 6b show the morphology of plane scanned position and EDS result of the worn tracks fabricated at the laser power of 1000 W. The elements Co, Cr, W, C, Ni, Si, Ti, Al, V, O and Mo are detected in the worn tracks, where the Co, Cr, W, C, Ni and Si come from the coating and account for 31.80wt% of total mass. While the Ti, Al and V come from the substrate and the O and Mo are the adsorption products of

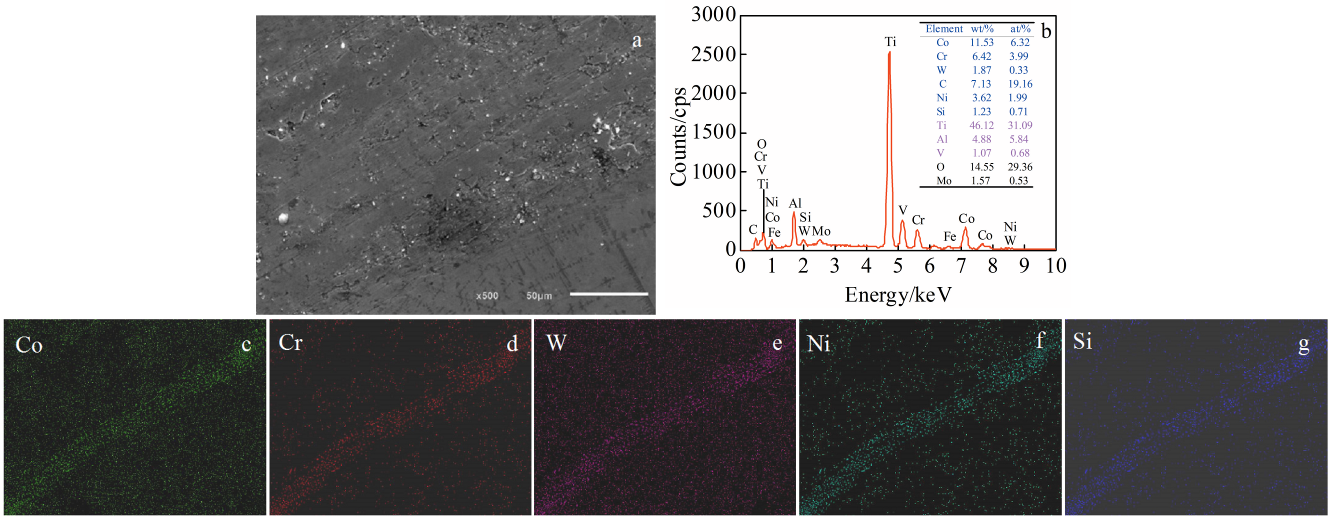

Fig.6 Morphology (a) and EDS analysis (b) of worn track fabricated at laser power of 1000 W; Co (c), Cr (d), W (e), Ni (f) and Si (g) element distributions in worn track

PAO+2.5%MoDTC oil. The Co, Cr, W, Ni and Si form the atoms-rich zones in the worn tracks, which improves the wear resistance of the substrate, as shown in Fig.6c~6g.

Fig.7a and 7b show the morphology of plane scanned position and EDS result of worn track fabricated at the laser power of 1200 W. The Co, Cr, W, C, Ni, Si, Ti, Al, V and S are detected in the worn track, where the Co, Cr, W, C, Ni and Si come from the coating and account for 47.53wt% of total mass. While the Ti, Al and V come from the substrate, and the S is the adsorption products of PAO+2.5%MoDTC oil. The mass fractions of Co, Cr, W, Ni and Si increase faster than those of coating fabricated at the laser power of 1000 W, which forms the bright atoms-rich zones in the worn track. It indicates that the wear resistance capacity is further reinforced, as shown in Fig.7c~7g.

Fig.8a and 8b show the morphology of plane scanned position and EDS result of worn track fabricated at the laser power of 1400 W. The Co, Cr, W, C, Ni, Si, Ti, Al, V, O and Mo are detected in the worn track, where the Co, Cr, W, C, Ni and Si account for 41.20wt% of total mass. While the Ti, Al and V come from the substrate, and the O and Mo are the adsorption products of PAO+2.5%MoDTC oil. The Co, Cr, W, Ni and Si form the atoms-rich zones in the worn tracks, which shows high wear resistance, as shown in Fig.8c~8g.

2.5 Morphologies and XRD analysis of worn tracks

To investigate the coating wear mechanism, the morpholo-

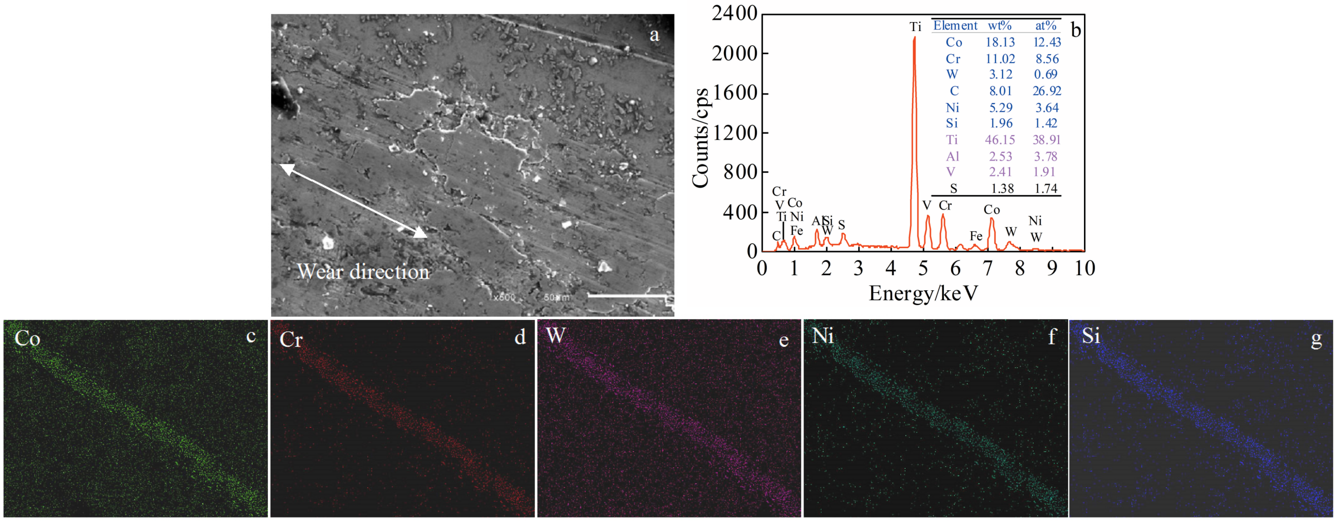

Fig.7 Morphology (a) and EDS analysis (b) of worn track fabricated at laser power of 1200 W; Co (c), Cr (d), W (e), Ni (f) and Si (g) element distributions in worn track

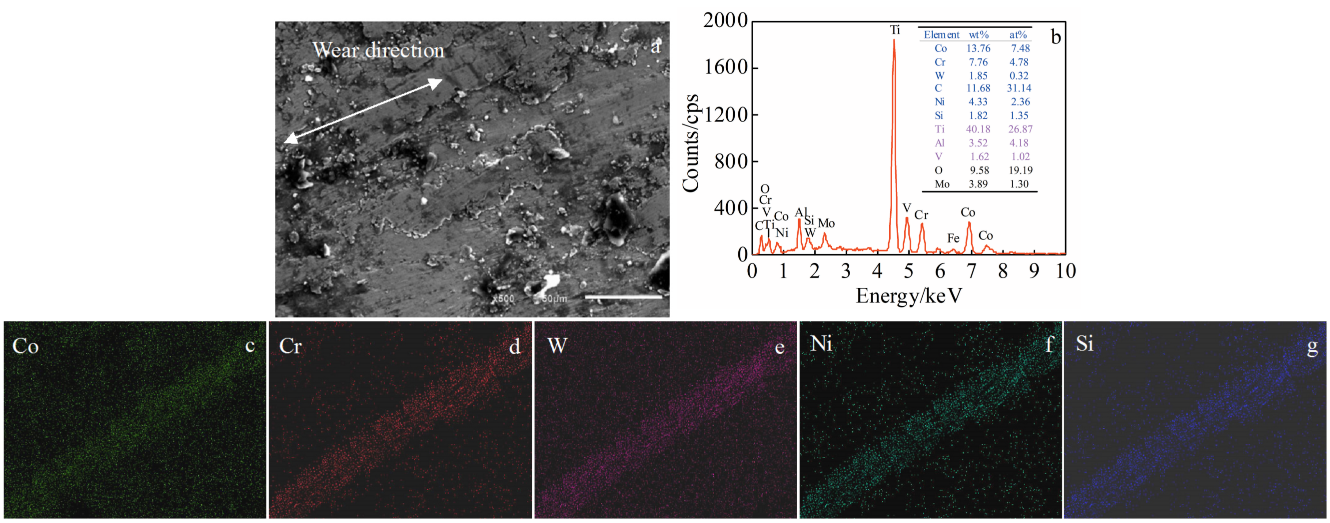

Fig.8 Morphology (a) and EDS analysis (b) of worn track fabricated at laser power of 1400 W; Co (c), Cr (d), W (e), Ni (f) and Si (g) element distributions in worn track

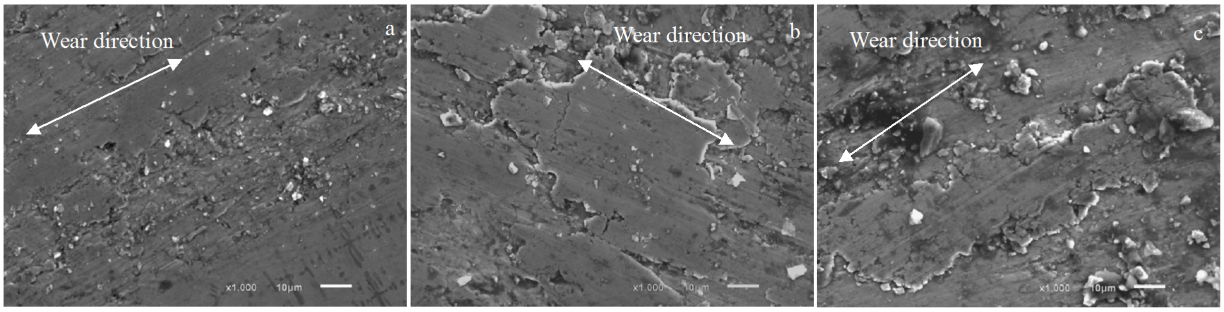

Fig.9 Morphologies of worn tracks fabricated at laser power of 1000 W (a), 1200 W (b) and 1400 W (c)

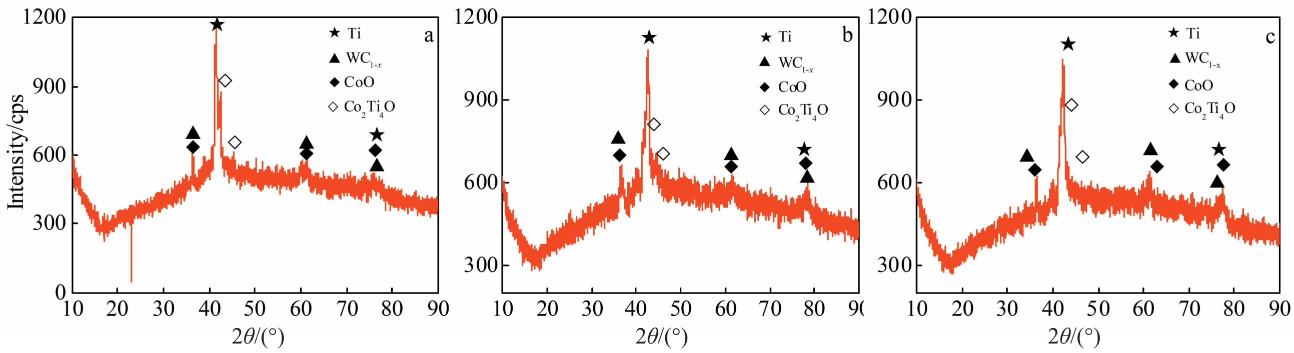

Fig.10 XRD patterns of worn tracks fabricated at laser power of 1000 W (a), 1200 W (b) and 1400 W (c)

gies and XRD analysis of worn tracks are shown in Fig.9 and Fig. 10. The plowing and cutting appear on the worn tracks, and the wear degree increases with the increase of laser power. The plowing grooves occur on the worn tracks owing to the high hardness, and the wear mechanism is abrasive wear, which is related with the hard intermetallic compounds of coatings[18]. The dendrite size plays a dominant role of anti-wear. Besides, the slight debris also appears on the worn tracks due to alternating stress during the wear test[19].

Fig.10 shows the XRD patterns of worn tracks fabricated at different laser powers. In the abrasive wear process, the hard phases are distributed in the coatings, which act as a role of wear resistance. The worn tracks fabricated at different laser powers are composed of Ti, WC_{1-x}, CoO and Co_2Ti_4O phases, among which the CoO and Co_2Ti_4O come from the oxidations during the LTS process. The phase composition of worn tracks shows no obvious difference from that of as-sprayed coatings, indicating that no new phase occurs during the wear test, and only the peak intensity decreases to some extent. From the above analyses, it can be seen that the laser power has slight effect on the phase composition of worn tracks, and the hard phases also play a secondary role of anti-wear.

3 Conclusions

1) The laser thermal sprayed $Co_{30}Cr_8W_{1.6}C_3Ni_{1.4}Si$ coatings are primarily composed of Ti, WC_{1-x}, CoO, Co_2Ti_4O and CoAl phases. The dendrite sizes increase with the increase of laser power, and the metallurgical bonding forms at the coating interface.

2) The average coefficient of friction of $Co_{30}Cr_8W_{1.6}C_3Ni_{1.4}Si$ coatings fabricated at the laser power of 1000, 1200 and 1400 W is 0.151, 0.120, and 0.171, respectively, and the corresponding wear rates are 1.17×10^{-6}, 1.33×10^{-6} and 2.80×10^{-6} $mm^3 \cdot N^{-1} \cdot m^{-1}$, respectively, which increase with the increase of laser power.

3) The wear mechanism of $Co_{30}Cr_8W_{1.6}C_3Ni_{1.4}Si$ coating is abrasive wear. The dendrite size is a dominant role of anti-wear performance, while the hard phase is the secondary influence factor of wear resistance.

References

1 Redmore E, Li X Y, Dong H S. *Wear*[J], 2019, 426-427: 952

2 Hatem A, Lin J L, Wei R H *et al*. *Surface and Coatings Technology*[J], 2018, 347: 1

3 Sun Y, Luo G Q, Zhang J *et al*. *Materials Science and Engineering A*[J], 2018, 736: 120

4 Imayev V M, Gaisin R A, Imayev R M. *Journal of Alloys and Compounds*[J], 2018, 762: 555

5 Li F Z, Guo B. *Journal of Alloys and Compounds*[J], 2018, 743: 576

6 Cai Z B, Cui X F, Liu Z *et al*. *Optics and Laser Technology*[J], 2018, 99(1): 276

7 Marin E, Offoiach R, Regis M *et al*. *Materials and Design*[J],

2016, 89: 314
8 Li Y S, Zhang C Z, Ma H T *et al*. *Materials Chemistry and Physics*[J], 2012, 134(1): 145
9 Zhou W T, Kong D J. *Surface and Coatings Technology*[J], 2019, 379: 125 058
10 Zhao W, Kong D J. *Applied Surface Science*[J], 2019, 481: 161
11 Zhang D H, Kong D J. *Applied Surface Science*[J], 2018, 457: 69
12 Zhao J, Gao Q W, Wang H Q *et al*. *Journal of Alloys and Compounds*[J], 2019, 785: 846
13 Yan H, Zhang J, Zhang P L *et al*. *Surface and Coatings Technology*[J], 2013, 232: 362
14 Li X, Zhang C H, Zhang S *et al*. *Optics and Laser Technology* [J], 2019, 114: 209
15 Okubo H, Tadokoro C, Sumi T *et al*. *Tribology International*[J], 2019, 133: 271
16 Zhang C, Liu L M, Xu H F *et al*. *Journal of Alloys and Compounds*[J], 2017, 727: 841
17 Weng F, Yu H J, Liu J L *et al*. *Optics and Laser Technology*[J], 2017, 92: 156
18 Ding L, Hu S S. *Surface and Coatings Technology*[J], 2015, 276: 565
19 Ocelík V, Matthews D, De Hosson J T M. *Surface and Coating Technology*[J], 2005, 197: 303

激光热喷涂 $Co_{30}Cr_8W_{1.6}C_3Ni_{1.4}Si$ 涂层在 PAO+2.5%MoDTC 油中摩擦学特性

徐健晏，孔德军

(常州大学 机械工程学院，江苏 常州 213164)

摘　要：为了提高TC4合金的耐磨性能，采用激光热喷涂技术在其表面制备了 $Co_{30}Cr_8W_{1.6}C_3Ni_{1.4}Si$ 涂层。通过扫描电子显微镜（SEM）和X射线衍射（XRD）分析了涂层的形貌和物相，并通过摩擦磨损实验研究了涂层在PAO+2.5%MoDTC（质量分数）油中的磨损行为。结果表明，激光热喷涂的 $Co_{30}Cr_8W_{1.6}C_3Ni_{1.4}Si$ 涂层主要由Ti、WC_{1-x}、CoO、Co_2Ti_4O 和CoAl相组成，在涂层界面形成冶金结合。在激光功率为1000、1200和1400 W时所制备的涂层平均摩擦因数分别为0.151、0.120和0.171，其对应的磨损率分别为 1.17×10^{-6}、1.33×10^{-6} 和 2.80×10^{-6} $mm^3\cdot N^{-1}\cdot m^{-1}$，磨损机理为磨粒磨损，其枝晶尺寸对降磨起主要作用。

关键词：激光热喷涂；$Co_{30}Cr_8W_{1.6}C_3Ni_{1.4}Si$ 涂层；PAO+2.5%MoDTC油；摩擦因数；磨损机理

作者简介：徐健晏，男，1993年生，硕士生，常州大学机械工程学院，江苏 常州 213164，E-mail：kong-dejun@163.com